Journal of Power Sources 180 (2008) 576–581

Contents lists available at ScienceDirect

Journal of Power Sources

journal homepage: www.elsevier.com/locate/jpowsour

Short communication

Li-ion transport kinetics in $LiMn_2O_4$ thin films prepared by radio frequency magnetron sputtering

J. Xie, T. Tanaka, N. Imanishi, T. Matsumura, A. Hirano, Y. Takeda*, O. Yamamoto

Department of Chemistry, Faculty of Engineering, Mie University, 1577 Kurimamachiya-cho, Tsu, Mie 514-8507, Japan

ARTICLE INFO

Article history:
Received 27 November 2007
Received in revised form 20 February 2008
Accepted 21 February 2008
Available online 4 March 2008

Keywords:
$LiMn_2O_4$ thin film
Radio frequency magnetron sputtering
Chemical diffusion coefficient
Cyclic voltammetry
Potentiostatic intermittent titration technique
Electrochemical impedance spectroscopy

ABSTRACT

$LiMn_2O_4$ thin films were deposited on silica glass substrates by radio frequency (RF) magnetron sputtering. The films were characterized by X-ray diffraction (XRD) and scanning electron microscope (SEM). Li-ion chemical diffusion coefficients $\tilde{D}_{Li}$ were measured by cyclic voltammetry (CV), potentiostatic intermittent titration technique (PITT), electrochemical impedance spectroscopy (EIS) and limiting current density (LCD). The $\tilde{D}_{Li}$ values depended on the content of Li in $Li_xMn_2O_4$. It was found that the $\tilde{D}_{Li}$ values by CV, PITT and LCD were in the order of 10^{-10}, 10^{-11} and 10^{-12} cm^2 s^{-1}, respectively, and those by EIS were in the range of 10^{-9} to 10^{-11} cm^2 s^{-1}. The $\tilde{D}_{Li}$ values obtained by above methods were compared with those by an electron blocking method. It turned out that the $\tilde{D}_{Li}$ values by the electron blocking method were more comparable with those by EIS.

© 2008 Elsevier B.V. All rights reserved.

1. Introduction

$LiMn_2O_4$ is one of the promising materials for Li-ion batteries due to its low cost, low toxicity and relatively high energy density. The kinetics of lithium ion transport through $LiMn_2O_4$ is a key factor determining the charge and discharge rate in a lithium ion battery with the $LiMn_2O_4$ cathode. Therefore, better understanding of the Li-ion chemical diffusion coefficient $\tilde{D}_{Li}$ in $LiMn_2O_4$ is of extreme importance for practical applications of this material. Previous research [1,2] on composite $LiMn_2O_4$ electrodes with a binder and a conducting additive as carbon showed that the chemical diffusion coefficients of this material were in the range of 10^{-9} to 10^{-8} cm^2 s^{-1}. However, it is difficult to determine the chemical diffusion coefficients accurately using the composite electrode because of the non-uniform potential distribution and unknown electrode surface area.

Compared with composite electrodes, a thin film electrode seems to be more appropriate for the measurement of diffusion coefficient since it has no conducting additive and no binder, and has a well-defined geometry. Comparative study of composite and thin film $LiMn_2O_4$ electrodes showed that the electronic contact between active material and current collector was better in the case of thin film electrodes [3], which is also essential for the accurate determination of diffusion kinetics. Up to now, many literatures have been available regarding the Li-ion chemical diffusion coefficient in $LiMn_2O_4$ thin films determined by electrochemical techniques such as cyclic voltammetry (CV) [4–9], galvanostatic intermittent titration technique (GITT) [4,8], potentiostatic intermittent titration technique (PITT) [7,10,11] and electrochemical impedance spectroscopy (EIS) [11,12–17]. However, the values of the Li-ion chemical diffusion coefficients determined by the above methods vary greatly, which depended on the measurement techniques and the sample preparation methods.

In this study, $LiMn_2O_4$ thin films were prepared by radio frequency (RF) magnetron sputtering. The Li-ion chemical diffusion coefficients in the thin films were measured using CV, PITT, EIS and LCD methods. To check the reliability of these measurement methods, an electron blocking technique using a lithium ion conducting polymer electrolyte was used to determine the ionic conductivity of $LiMn_2O_4$ material. The chemical diffusion coefficients were calculated from the ionic conductivities using the Nernst-Einstein equation and were compared with those determined by the different measurement methods.

2. Experimental

The $LiMn_2O_4$ thin films were deposited on silica glass substrates (8 mm × 8 mm) by RF magnetron sputtering. Gold was pre-deposited on the substrate by RF magnetron sputtering in pure Ar for 60 min as a current collector. The target (50 mm in

* Corresponding author. Tel.: +81 59 231 9421; fax: +81 59 231 9419.
E-mail address: takeda@chem.mie-u.ac.jp (Y. Takeda).

0378-7753/$ – see front matter © 2008 Elsevier B.V. All rights reserved.
doi:10.1016/j.jpowsour.2008.02.049

diameter) used for sputtering was prepared by cold pressing a commercial $LiMn_2O_4$ powder (Housen, Japan). The $LiMn_2O_4$ sputtering was carried out for 8 h in an Ar/O_2 mixture ($Ar/O_2 = 7/3$) with a working pressure of 0.4 Pa. The power used for the $LiMn_2O_4$ sputtering was 30 W, and the distance between the substrate and the target was 10 cm. Prior to the $LiMn_2O_4$ sputtering, the target was pre-sputtered for 15 min under the same conditions, in order to eliminate impurities. The as-prepared $LiMn_2O_4$ thin films were then annealed at 700 °C for 30 min in air to improve crystallization. The crystal structure of the films was characterized by X-ray diffraction (XRD) using a RINT2000/PC diffract meter with Cu Kα radiation. The surface and cross-section morphology of the $LiMn_2O_4$ thin films were observed by scanning electron microscope (SEM) using a Hitachi S-4000.

Electrochemical measurements of the $LiMn_2O_4$ thin films (active area of 0.64 cm^2) were performed using three-electrode beaker cells. The cells were assembled in an Ar-filled glove box using Li foil as the counter and the reference electrodes. The electrolyte used was 1 M $LiClO_4$ in a mixture (1:1 in volume) of ethylene carbonate (EC)/diethylene carbonate (DEC). Galvanostatic cycling test of the cells was carried out at a current of 5 μA between 3 and 4.2 V. The CV measurement was performed between 3 and 4.3 V at scan rates ranging from 0.5 to 10 mV s^{-1} using a Solartron 1287 electrochemical interface. For the PITT measurements, a potential step of 10 mV was applied and the current was recorded as a function of time. The potential was stepped to the next level when the current decreased to below 0.1 μA cm^{-2}. The procedure was repeated between 3.89 and 4.2 V. EIS measurements were conducted at various electrode potentials by applying an AC signal of 10 mV amplitude over the frequency range from 1 MHz to 1 mHz using a Solartron 1287 electrochemical interface combined with a Solartron 1260 frequency response analyzer. All the electrochemical measurements were performed at room temperature. To check the reliability of these methods, chemical diffusion coefficients obtained were compared with those measured by the electron blocking method using a lithium ion conducting polymer electrolyte. A dc current was passed into a cell Li/polymer electrolyte/$Li_xMn_2O_4$/polymer electrolyte/Li, and the cell resistance was measured. The solid polymer electrolyte was prepared using the previously reported method [18]. Polyethylene oxide (PEO, Aldrich, molecular weight = 6×10^5) and $Li(CF_3SO_2)_2N$ (Fluka Chemical) were dissolved in CH_3CN in the Ar-filled glove box, and the slurry was cast onto a Teflon plate, followed by drying at 120 °C under vacuum for 12 h. The content of Li in PEO–$Li(CF_3SO_2)_2N$ was Li/O = 1/18. The Li deficient compositions $Li_{0.58}Mn_2O_4$ and $Li_{0.82}Mn_2O_4$ were prepared by a chemical oxidation method using Br_2 as the oxidative agent [19]. The compositions of the oxidized samples were determined by inductively coupled radio frequency plasma (ICP) spectroscopy, using a Shimadzu ICPS-1000IV spectrometer. The tablets for dc polarization measurements were prepared by pressing the powder without adding any binder and conducting agent. The compositions of the as received powder and the sputtered film are $Li_{1.08}Mn_{1.9}O_4$ and $Li_{1.03}Mn_{1.9}O_4$, respectively, as checked by ICP. For simplicity, we use $LiMn_2O_4$ instead of $Li_{1.08}Mn_{1.9}O_4$ or $Li_{1.03}Mn_{1.9}O_4$ in the following sections.

3. Results and discussion

Fig. 1 shows the XRD patterns of the $LiMn_2O_4$ thin film prepared by RF magnetron sputtering followed by annealing in air at 700 °C for 30 min. For comparison, the XRD pattern of the $LiMn_2O_4$ powder is also given in Fig. 1. It can be seen that all the diffraction peaks can be indexed to the spinel $LiMn_2O_4$ without any phase impurities.

Fig. 2 shows the morphology of surface and cross-section of the $LiMn_2O_4$ thin film prepared by RF magnetron sputtering. As seen in the figure, the film is dense, uniform and well adherent to the substrate. These properties are necessary for the accurate characterization of Li-ion diffusion kinetics. The thickness of the $LiMn_2O_4$ thin film is about 0.6 μm as estimated from the cross-section morphology of the film. A density of around 95% is estimated by comparing the calculated and observed thickness of the $LiMn_2O_4$ thin film.

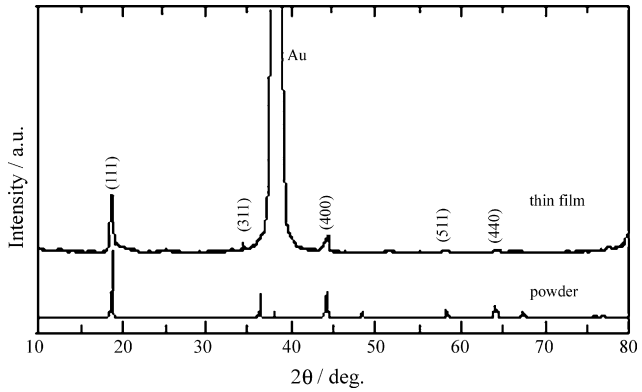

Fig. 1. XRD patterns of the $LiMn_2O_4$ thin film prepared by RF magnetron sputtering.

Fig. 3 gives a typical charge and discharge curve of the $LiMn_2O_4$ thin film at a constant current of 5 μA in a potential range 3–4.2 V. The voltage profiles exhibit two expected potential plateaus at around 4 and 4.2 V. This potential profile shows a good agreement with the previously reported results. The specific capacity of the thin film is calculated to be about 80 mA h g^{-1} from the weight gain of the substrate after sputtering. The obtained $LiMn_2O_4$ thin film

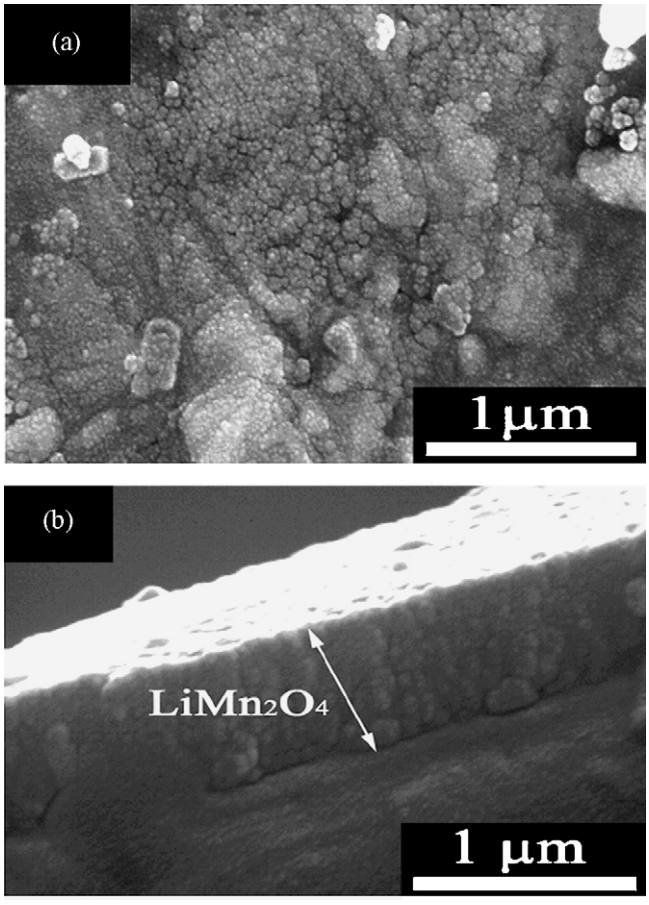

Fig. 2. SEM images of the $LiMn_2O_4$ thin film prepared by RF magnetron sputtering: (a) surface and (b) cross-section.

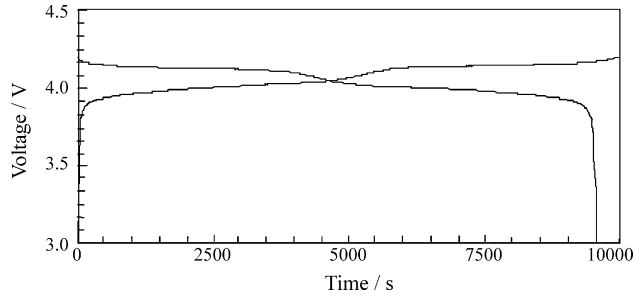

Fig. 3. A typical charge and discharge curve of $LiMn_2O_4$ thin film.

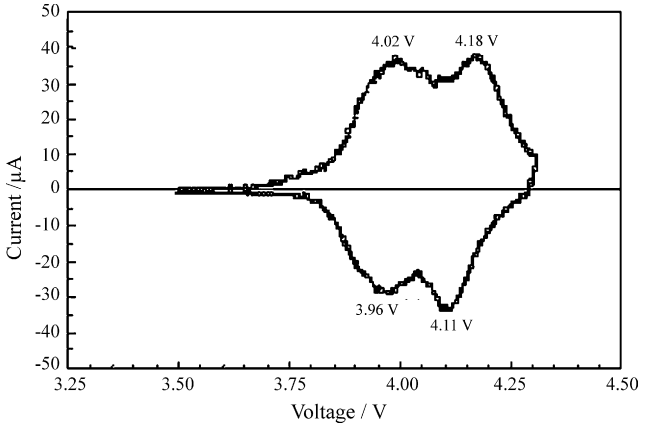

Fig. 4. CV of the $LiMn_2O_4$ thin film at a scan rate of 0.5 mV s^{-1}.

is well crystallized and is suitable for the Li-ion diffusion kinetics characterization.

Fig. 4 shows the CV curve of the $LiMn_2O_4$ thin film at a scan rate of 0.5 mV s^{-1}. Note that two sets of well-separated peaks can be clearly seen, which correspond to the potential plateaus in Fig. 3. The peaks located at 4.02 and 4.18 V during cathodic scan correspond to the two successive steps of Li ions deintercalation from $LiMn_2O_4$ to form λ-MnO_2, while the peaks located at 3.96 and 4.11 V during anodic scan correspond to Li ions intercalation into λ-MnO_2 to form $LiMn_2O_4$ [20–22]. The CV behavior of the $LiMn_2O_4$ thin film is in good agreement with the previous report on $LiMn_2O_4$ thin films [8,23–25].

Fig. 5 shows the CV curves of the $LiMn_2O_4$ thin film at different scan rates. Note that, the peak current (I_p) increases with increasing scan rate, and the cathodic peaks shift to lower potential and the anodic peaks to higher potential with increasing scan rate. In addition, at a high scan rate (>2 mV s^{-1}), the two cathodic peaks combine into one peak, and the anodic peak at 4.18 V disappears gradually. Therefore, only the anodic peak at 4.02 V is used to characterize the Li-ion diffusion kinetics in the $LiMn_2O_4$ thin film. As seen in the inset of Fig. 5, when the scan rate is over 1 mV s^{-1}, I_p exhibits a linear relationship with the square root of the scan rate ($v^{1/2}$), which is expected for a diffusion-controlled process. The relation is known as a typical Randles-Sevcik relation, which is expressed as [9,25]:

$$I_p = 0.4463 n^{3/2} F^{3/2} C_{Li} S R^{-1/2} T^{-1/2} \tilde{D}_{Li}^{1/2} v^{1/2} \quad (1)$$

where n is the charge transfer number, F the Faraday constant, C_{Li} the Li-ion concentration, S the surface area of the electrode, R the gas constant and T the absolute temperature (K). The $\tilde{D}_{Li}$ value calculated from Eq. (1) is 1.2×10^{-10} cm^2 s^{-1} for the $LiMn_2O_4$ thin film. Singh et al. [5] also used CV to measure $\tilde{D}_{Li}$ values of $LiMn_2O_4$ thin film prepared by pulsed laser deposition (PLD). They found that the film showed a $\tilde{D}_{Li}$ value of 5.379×10^{-10} cm^2 s^{-1}. Low $\tilde{D}_{Li}$ values as 10^{-12} and 10^{-11} cm^2 s^{-1} were observed for the $LiMn_2O_4$ thin film prepared also by PLD [8] and by spin coating method [9], respectively. By the CV method, the dependence of $\tilde{D}_{Li}$ on the content of x in $Li_xMn_2O_4$ cannot be measured, but only the averaged $\tilde{D}_{Li}$ in $Li_xMn_2O_4$ is observed.

The PITT method is useful to determine the chemical diffusion coefficient of the sample with different x in $Li_xMn_2O_4$. Fig. 6 shows a typical time dependence of the transient current for the $LiMn_2O_4$ thin film, where a potential step from 3.89 to 3.90 V was applied between the $LiMn_2O_4$ electrode and the Li reference electrode. The time (t) dependence of the transient current (I_t) at each potential step can be expressed by the following equation [26]:

$$I_t = \frac{2FS(C_s - C_0)\tilde{D}_{Li}}{L} \exp\left(-\frac{\pi^2 \tilde{D}_{Li} t}{4L^2}\right) \quad (2)$$

where F is the Faraday constant, S the surface area of the electrode, $C_s - C_0$ the concentration difference at the surface at time t and at time $t = 0$ during each potential step and L the thickness of the film. $\tilde{D}_{Li}$ can be calculated from the slope of the linear region in the Ln (I_t) vs. t plot shown in the inset of Fig. 6 using the following equation [26]:

$$\tilde{D}_{Li} = -\frac{d\mathrm{Ln}(I_t)}{dt} \frac{4L^2}{\pi^2} \quad (3)$$

The chemical diffusion coefficient calculated using Eq. (3) is 4.6×10^{-11} cm^2 s^{-1} during the potential step from 3.89 to 3.90 V,

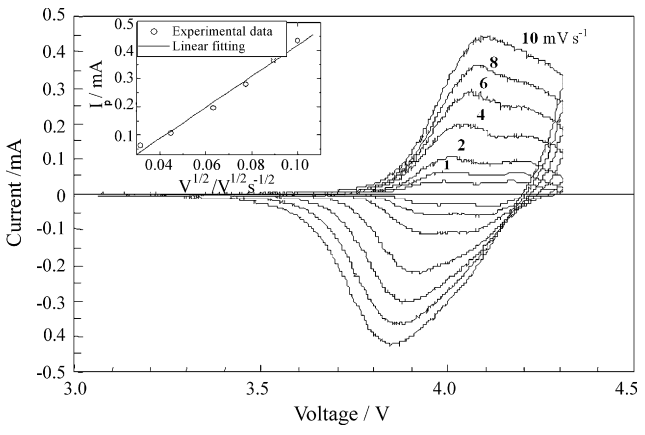

Fig. 5. CV curves at scan rates ranging from 0.5 to 10 mV s^{-1}. The inset shows the peak current I_p vs. the square root of the scan rate, $v^{1/2}$.

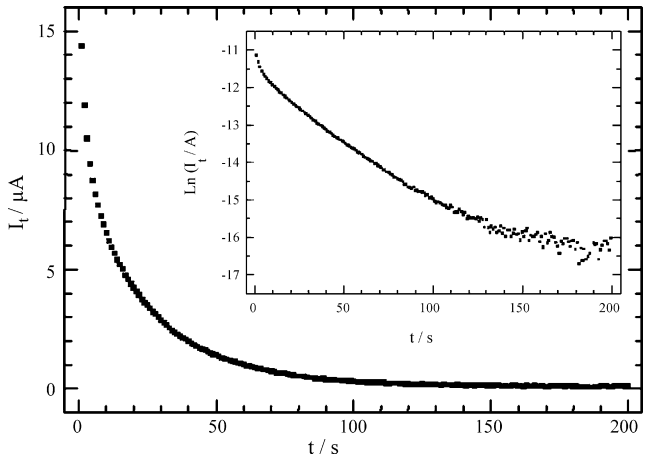

Fig. 6. Time dependence of the transient current I_t when the potential is increased from 3.89 to 3.90 V. The inset shows the Ln (I_t/A) vs. t.

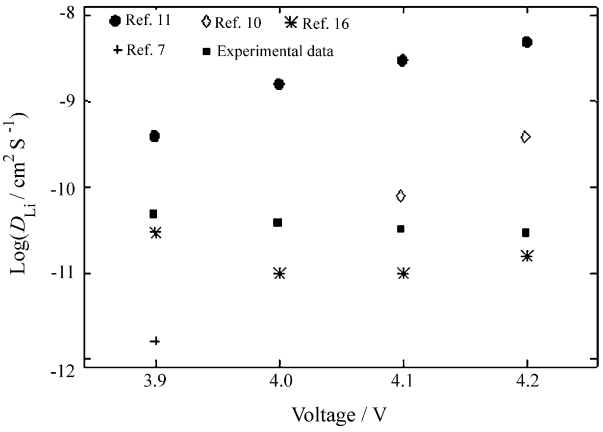

Fig. 7. Electrode potential dependence of chemical diffusion coefficients by PITT.

where the thickness of the sample was estimated from the SEM image as 600 nm. The chemical diffusion coefficients depend on the electrode potential of the $Li_xMn_2O_4$ film and the dependence is shown in Fig. 7 along with the previously reported $\tilde{D}_{Li}$ values of the $Li_xMn_2O_4$ thin films [7,10,11,16], which were also measured by the PITT method. As shown in Fig. 7, the thin films prepared by the same preparation technique exhibit the different values of $\tilde{D}_{Li}$. Some data are comparable and some are far from our results.

The EIS method is also considered to be useful to identify the chemical diffusion coefficient. Fig. 8(a) shows a typical Nyquist plot for the film with the electrode potential 3.9 V vs. Li^+/Li. The plot consists of a semicircle in a high frequency region, a straight line with a slope of approximately 45° in a medium frequency region, and a steeper straight line in a low frequency region. The high-frequency semicircle is attributed to a charge-transfer process, the straight line of 45° slope is related to the Warburg region associated with Li-ion solid phase diffusion in the bulk $LiMn_2O_4$ thin film, and the steeper straight line corresponds to the onset of finite length diffusion. The equation for $\tilde{D}_{Li}$ measured by EIS can be expressed as [27]:

$$\tilde{D}_{Li} = \frac{1}{2}\left[\left(\frac{V_m}{FS\sigma}\right)\left(\frac{dE}{d\delta}\right)\right]^2 \quad (4)$$

where V_m is the molar volume of $LiMn_2O_4$, F the Faraday constant, S (cm^2) the surface area of the electrode, σ ($\Omega\,Hz^{1/2}$) the Warburg factor and $dE/d\delta$ (V) the slope of the electrode potential (E) vs. composition (δ). The chemical diffusion coefficient depends on the Warburg factor, σ, in the Warburg region, which can be determined by linearly fitting the Z' vs. $\omega^{-1/2}$ plot. Fig. 8(b) shows the relationship between Z' and the angular frequency, ω, in the Warburg region at this potential. The chemical diffusion coefficient of the $LiMn_2O_4$ thin film at 3.9 V is calculated to be 1.6×10^{-9} cm^2 s^{-1} from Eq. (4). The $\tilde{D}_{Li}$ values at 4.0 and 4.1 V are calculated to be 4.3×10^{-11} and 5.5×10^{-11} cm^2 s^{-1}, respectively. These values are plotted in Fig. 9 along with those reported previously [11,13,15], which were measured also by the EIS method. The thin films prepared by a spin coating method [11] show higher $\tilde{D}_{Li}$ and those prepared by an electrostatic deposition method [14,15] are comparable with our results. The high $\tilde{D}_{Li}$ values may be due to the unsuitable microstructure to measure the chemical diffusion coefficient.

According to the diffusion control electrochemical reaction process, the chemical diffusion coefficient can be obtained using the following equation [28]:

$$\tilde{D}_{Li} = \frac{I_l L}{nFC_{Li}} \quad (5)$$

where I_l is the limiting current density, L the thickness of the film, F the Faraday constant, C_{Li} the Li-ion concentration and n the charge of diffusion ions. Fig. 10 shows an equilibrium potential vs. applied current curve, where a constant current was passed at a starting cell voltage 3.9 V and the equilibrium cell voltage measured. After the steady cell voltage, the cell was discharged to 3.9 V again and a high current was passed. Note that when the current density is close to 140 μA, the equilibrium potential increases steeply, where the composition of the thin film was around $Li_{0.5}Mn_2O_4$. The chemical diffusion coefficients obtained by above method was

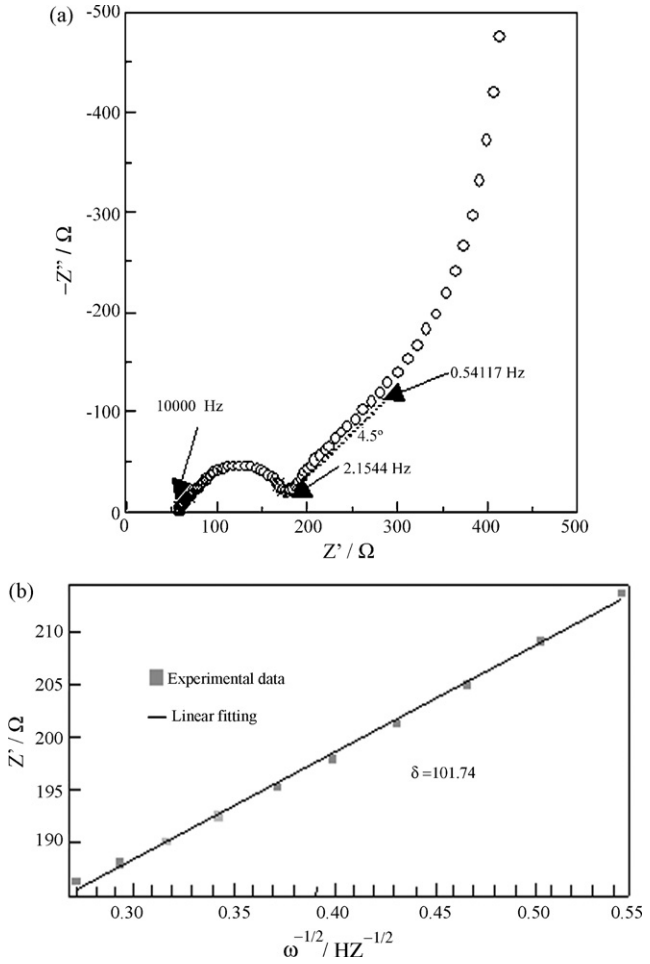

Fig. 8. Nyquist plot of $LiMn_2O_4$ thin film at 3.9 V (a) and Z' vs. $\omega^{-1/2}$ in the Warburg region (b).

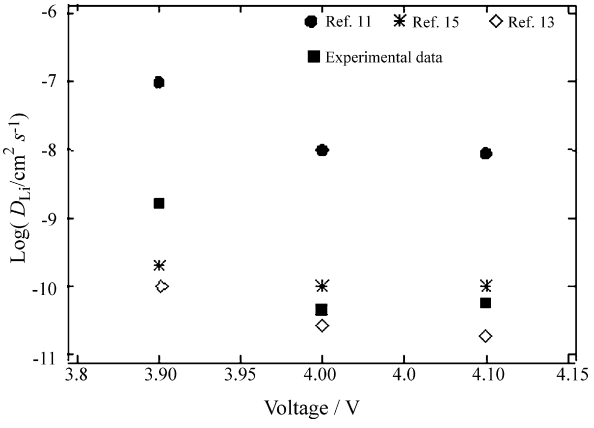

Fig. 9. Electrode potential dependence of chemical diffusion coefficients by EIS.

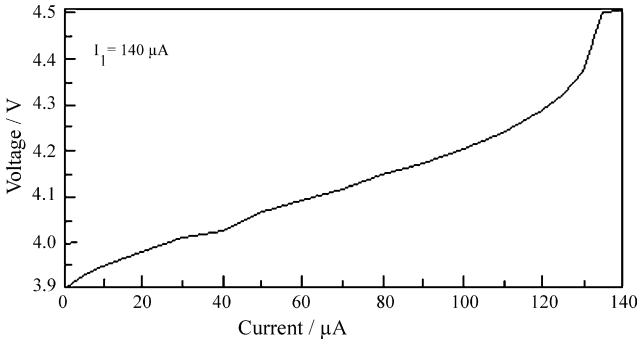

Fig. 10. Equilibrium potential as a function of applied current density starting at 3.9 V of the $LiMn_2O_4$ thin film.

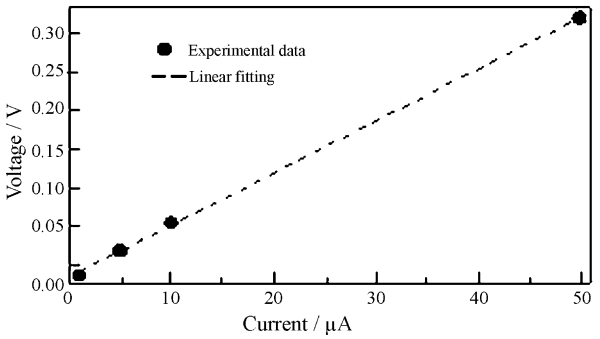

Fig. 11. Equilibrium voltage vs. polarization current at 70 °C for a Li/polymer electrolyte/$LiMn_2O_4$/polymer electrolyte/Li cell.

3.6×10^{-12} cm^2 s^{-1}.

According to the Nernst-Einstein equation [29], the ionic conductivity σ_i can be expressed as

$$\sigma_i = \frac{Z^2F^2\tilde{D}_{self}N_{Li}}{RT} \quad (6)$$

where Z is the charge number, F the Faraday constant, $\tilde{D}_{self}$ the self-diffusion coefficient, N_{Li} the number of ion pairs per unit volume, R the gas constant and T the absolute temperature. The chemical diffusion coefficient $\tilde{D}_{Li}$ is related with self-diffusion coefficient by the following equations [30,31]:

$$\tilde{D}_{Li} = \tilde{D}_{self}\phi \quad (7)$$

$$\phi = -\frac{F\delta}{RT}\frac{dE}{d\delta} \quad (8)$$

where $dE/d\delta$ is the slope of the electrode potential vs. the composition curve obtained from Fig. 3. That is, the chemical diffusion coefficients can be estimated from the lithium ion conductivity in $Li_xMn_2O_4$. The electrical conductivity of $Li_xMn_2O_4$ was reported to be about 10^{-3} S cm^{-1} at room temperature [32], which consists of electronic and ionic conductivity. The ionic conductivity of the electron and ion mixed conductor was measured with the help of the electron blocking method using a pure ionic conductor [33]. In the present study, PEO–$Li(CF_3SO_2)_2N$ (Li/O = 1/18) was used as pure lithium ion conductivity solid electrolyte. The conductivity of the polymer was about 4×10^{-4} S cm^{-1} at 60 °C and 5×10^{-6} S cm^{-1} at 25 °C [18]. The lithium ion conductivity of $LiMn_2O_4$ was measured using a symmetric cell Li/PEO–$Li(CF_3SO_2)_2N$/$Li_xMn_2O_4$/PEO–$Li(CF_3SO_2)_2N$/Li in a temperature range of 50–70 °C and was extrapolated to room temperature, because the ionic conductivity of PEO-based electrolyte was too low to measure the ionic conductivity of $Li_xMn_2O_4$. The pressed tablets of $LiMn_2O_4$ and Li deficient $Li_{0.58}Mn_2O_4$ and $Li_{0.82}Mn_2O_4$ were used for the ionic conductivity measurement. The Li deficient samples were prepared by a chemical oxidation method and the ratio of Li/Mn was determined by ICP analysis. A typical result of the equilibrium cell voltage and the current curve at 70 °C for $LiMn_2O_4$ is shown in Fig. 11. The curve exhibits a good linear relationship and the ionic resistance, R, can be obtained from the slope of the fitting line. Therefore, the ionic conductivity, σ_i, can be determined by the following equation:

$$\sigma_i = \frac{d}{RS} \quad (9)$$

where d, R and S denote the thickness, the resistance and the surface area of the sample tablet, respectively. The ionic conductivity of $LiMn_2O_4$ at room temperature extrapolated from the conductivity data at 70, 60 and 50 °C is 5.25×10^{-7} S cm^{-1} at 25 °C using the Arrhenius equation:

$$\sigma_i = A \exp\left(-\frac{E_a}{RT}\right) \quad (10)$$

where A is the pre-exponential factor and E_a the activation energy for Li-ion conduction. The lithium ion conductivities of $Li_{0.58}Mn_2O_4$ and $Li_{0.82}Mn_2O_4$ were measured to be 1.05×10^{-7} and 9.57×10^{-7} S cm^{-1}, respectively, by the same method.

The $\tilde{D}_{Li}$ values of $Li_xMn_2O_4$ obtained by the different techniques are summarized in Table 1 and Fig. 12 summarizes the dependence of $\tilde{D}_{Li}$ on the electrode potential of $Li_xMn_2O_4$, where the electrode potential of $LiMn_2O_4$, $Li_{0.82}Mn_2O_4$ and $Li_{0.58}Mn_2O_4$ was estimated from the previously reported electrode potentials vs. lithium content curves [34,35]. It is interesting to note that the $\tilde{D}_{Li}$ values calculated by ionic conductivity are very close to those by

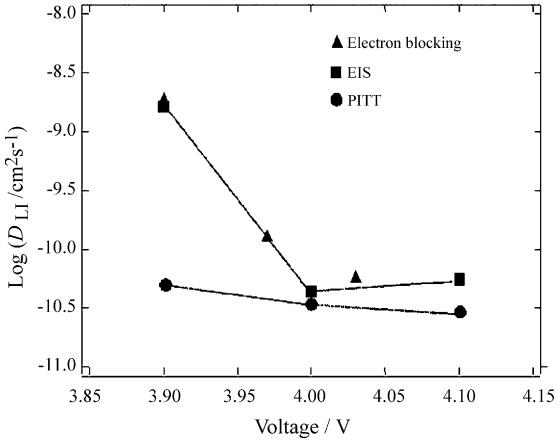

Fig. 12. Comparison of chemical diffusion coefficients by electron blocking, PITT and EIS.

Table 1
$\tilde{D}_{Li}$ values of $Li_xMn_2O_4$ thin films at various potentials by different methods

Potential vs. Li^+/Li (V)	PITT (cm^2 s^{-1})	EIS (cm^2 s^{-1})	LCD (cm^2 s^{-1})	CV (cm^2 s^{-1})	Ionic conductivity (cm^2 s^{-1})
3.9	4.6×10^{-11}	1.6×10^{-9}			$x = 1.00$, 1.9×10^{-9}
4.0	3.6×10^{-11}	4.3×10^{-11}	$x = 0.5$	1.2×10^{-10}	$x = 0.82$, 1.3×10^{-10}
4.1	3.1×10^{-11}	5.5×10^{-11}	3.7×10^{-12}		$x = 0.58$, 5.9×10^{-11}
4.2	2.8×10^{-11}	–			–

EIS (Fig. 12). Apart from the value at 3.9 V, the values at other potentials are in the same order with those by PITT and also comparable with that by CV. It is suggested that the $\tilde{D}_{Li}$ values by EIS are more reliable compared with those by other methods. The low $\tilde{D}_{Li}$ values by LCD may be due to second phase on $Li_xMn_2O_4$.

4. Conclusions

The $LiMn_2O_4$ thin films were prepared by RF magnetron sputtering on silica glass substrates. The films show good crystallization after annealing at 700 °C for 30 min. The Li-ion diffusion kinetics in the $LiMn_2O_4$ films was characterized by CV, PITT, EIS and LCD. The ionic conductivity of the $Li_xMn_2O_4$ was determined by the electron blocking method. The lithium ion conductivities of $Li_{0.58}Mn_2O_4$ and $Li_{0.82}Mn_2O_4$ are 1.05×10^{-7} and 9.57×10^{-7} S cm^{-1}, respectively, as measured by this method. The $\tilde{D}_{Li}$ values by PITT and EIS are good agreement with those by the electron blocking method, except for that at 3.9 V by PITT. We can conclude that the chemical diffusion coefficients of $Li_xMn_2O_4$ are $1.6 - 1.9 \times 10^{-9}$ cm^2 s^{-1} at 3.9 V, $3.6–4.3 \times 10^{-11}$ cm^2 s^{-1} at 4.0 V and $3.1–5.5 \times 10^{-11}$ cm^2 s^{-1} at 4.1 V.

Acknowledgements

This research work was carried out under a collaboration program of Mie University and Genesis Research Institute, Nagoya, Japan.

References

[1] D. Guyomard, J.M. Tarascon, J. Electrochem. Soc. 139 (1992) 937.
[2] J. Barker, R. Pynenburg, R. Koksbang, J. Power Sources 52 (1994) 185.
[3] A.K. Hjelm, G. Lindbergh, Electrochim. Acta 47 (2002) 1747.
[4] K.A. Striebel, C.Z. Deng, S.J. Wen, E.J. Cairns, J. Electrochem. Soc. 143 (1996) 1821.
[5] D. Singh, W.S. Kim, V. Cracium, H. Hofmann, P.K. Singh, Appl. Surf. Sci. 197/198 (2002) 516.
[6] Y.H. Rho, K. Kanamura, J. Electroanal. Chem. 559 (2003) 69.
[7] F.Y. Shih, K.Z. Fung, J. Power Sources 159 (2006) 179.
[8] C. Julien, E. Haro-Poniatowski, M.A. Camacho-Lopez, L. Escobar-Alarcon, J. Jimenez-Jarquin, Mater. Sci. Eng. B 72 (2000) 36.
[9] X.M. Wu, Z.Q. He, S. Chen, M.Y. Ma, Z.B. Xiao, J.B. Liu, Mater. Chem. Phys. 105 (2007) 58.
[10] F. Cao, J. Prakash, Electrochim. Acta 47 (2002) 1607.
[11] Y.H. Rho, K. Dokko, K. Kanamura, J. Power Sources 157 (2006) 471.
[12] K.A. Striebel, A. Rougier, C.R. Horne, R.P. Reade, E.J. Cairns, J. Electrochem. Soc. 146 (1999) 4339.
[13] M. Mohamedi, D. Takahashi, T. Uchiyama, T. Itoh, M. Nishizawa, I. Uchida, J. Power Sources 93 (2001) 93.
[14] M. Mohamedi, D. Takahashi, T. Itoh, I. Uchida, Electrochim. Acta 47 (2002) 3483.
[15] M. Mohamedi, D. Takahashi, T. Itoh, M. Umeda, I. Uchida, J. Electrochem. Soc. 149 (2002) A19.
[16] D. Shu, K.Y. Chung, W.I. Cho, K.B. Kim, J. Power Sources 114 (2003) 253.
[17] S.B. Tang, M.O. Lai, L. Lu, J. Power Sources 164 (2007) 372.
[18] Q. Li, H.Y. Sun, Y. Takeda, N. Imanishi, J. Yang, O. Yamamoto, J. Power Sources 94 (2001) 201.
[19] K. Uchiyam, Y. Takeda, N. Imanishi, O. Yamamoto, M. Tabuchi, J. Jpn. Soc. Powder Powder Metall. 47 (2000) 183.
[20] J.M. Tarascon, E. Wang, F.K. Shokoohi, W.R. Mckinnon, S. Colson, J. Electrochem. Soc. 138 (1991) 2859.
[21] F.K. Shokoohi, J.M. Tarascon, B.J. Wilkens, D. Guyomard, C.C. Chang, J. Electrochem. Soc. 139 (1992) 1845.
[22] J.M. Tarascon, F. Coowar, G. Amatucci, F.K. Shokoohi, D. Guyomard, J. Power Sources 54 (1995) 103.
[23] A. Rougier, K.A. Striebel, S.J. Wen, E.J. Cairns, J. Electrochem. Soc. 145 (1998) 2975.
[24] K.F. Chiu, H.C. Lin, K.M. Lin, C.H. Tsai, J. Electrochem. Soc. 152 (2005) A2058.
[25] S.B. Tang, M.O. Lai, L. Lu, J. Alloy Comp. 449 (2008) 300.
[26] C.J. Wen, B.A. Boukamp, R.A. Huggins, W. Weppner, J. Electrochem. Soc. 126 (1979) 2258.
[27] C. Ho, I.D. Raistrick, R.A. Huggins, J. Electrochem. Soc. 127 (1980) 345.
[28] W. Weppner, R. Huggins, J. Electrochem. Soc. 124 (1977) 1569.
[29] N.F. Mott, R.W. Gurney, Electronic Processes in Ionic Crystals, Oxford, 1940.
[30] Y.I. Jang, B.J. Neudecker, N.J. Dudney, Electrochem. Solid-State Lett. 4 (2001) A74.
[31] L.A. Montoro, J.M. Rosolen, Electrochim. Acta 49 (2004) 3243.
[32] L.Q. Chen, J. Schoonman, Solid State Ionics 67 (1994) 17.
[33] T. Takahashi, O. Yamamoto, J. Electrochem. Soc. 119 (1972) 1736.
[34] S.I. Pyun, S.W. Kim, J. Power Sources 97–98 (2001) 371.
[35] H. Abiko, M. Hibino, T. Kudo, J. Power Sources 124 (2003) 526.